Soils and Rocks
An International Journal of Geotechnical and Geoenvironmental Engineering
www.soilsandrocks.com
ISSN 1980-9743
ISSN-e 2675-5475

# Finite element prediction of long-term behaviour of a test embankment based on back-analysis of early stages

Fernando da Silva Oliveira[1#], Francisco de Rezende Lopes[2]

Case Study

**Keywords**
Embankment on soft clay
Settlements
Horizontal displacements
Soft clay
Consolidation
Numerical modelling

**Abstract**

The paper presents the finite element modeling of a test embankment built at one of the construction sites of the 2016 Olympic Games in Rio de Janeiro, Brazil. The embankment was raised over 6 weeks to a height of 6.7 m, and was monitored during construction and in the following month. The experiment had to end after a month of measurements due to the need to develop the test area. Instrumentation consisted of electric piezometers, settlement plates and inclinometers. The subsoil featured a pack of sedimentary soils, including soft clays. Firstly, field and laboratory tests were evaluated for numerical modelling parameters, and a sensitivity study of the various parameters was carried out. Program PLAXIS was used with the most suitable soil models for the different soil layers. The time-dependent behaviour of the clayey layers followed Terzaghi's consolidation theory for pore pressure dissipation coupled with a Buisman (1936)-type solution for viscous behaviour. The final analysis used parameters adjusted by back-analysis of measurements in the monitoring period (2.5 months) in a 3D model. This analysis was extended to 50 years, aiming to predict the long-term behaviour of the embankment. Results of the 50-year analysis indicated that after 20 years the excess pore pressures would have practically dissipated, but that the long-term settlement would be 2.5 times greater than that at the end of construction. Furthermore, the ground horizontal displacement would be about 4 times greater than that measured at the end of construction.

## 1. Introduction

An embankment was needed to raise the grade of the construction site of the Athletes' Village of the 2016 Olympic Games in Rio de Janeiro, Brazil. There were concerns about both the long-term settlements of the embankment and the horizontal displacements it could induce on nearby foundations. A test embankment was raised over 6 weeks to a height of 6.7 m and was monitored during construction and in the subsequent month. Due to the construction schedule of the entire project, monitoring could not be extended further. Instrumentation consisted of electric piezometers, settlement plates and inclinometers. The local ground conditions featured a pack of sedimentary soils, including soft clays. Firstly, field and laboratory tests were evaluated for numerical modelling parameters; secondly, a sensitivity study of the various parameters was carried out with a 2D model with program PLAXIS. Third, a 3D model was run with the average parameters, and the most sensitive of them were further adjusted to match measurements in the monitoring period (2.5 months). With these parameters, a long-term (3D) analysis was performed in order to predict the long-term behaviour of the embankment.

The time-dependent behaviour of clayey soils is related to two phenomena: consolidation (of hydrodynamic nature) and creep (of viscous nature). The first rational approach to the consolidation phenomenon was proposed by Terzaghi (1923), for 1D strains and constant excess pore pressure with depth. In the following years, different authors proposed extensions of this theory, such as 3D conditions, excess pore pressures not constant with depth, coupling pore-pressure dissipation with stresses, large strains etc., but respecting the effective stress principle – i.e., not considering creep. However, a few years after the publication of Terzaghi's theory, experimental results began to reveal that an additional phenomenon existed, the most evident indication being a straight slope of the $\varepsilon$ vs. log $t$ curve – instead of a horizontal asymptote – at the end of the load stages in oedometer tests. This additional phenomenon was termed as "secular effect" (Buisman, 1936) or "secondary time effect" (Gray, 1936) and, in fact, is a manifestation of the viscous nature of soils. The most widespread theory for the prediction of viscous

#Corresponding author. E-mail address: fsilvaoliveira@gmail.com
[1]Transpetro, Manutenção de Faixas de Dutos RJMG, Duque de Caxias, RJ, Brasil.
[2]Universidade Federal do Rio de Janeiro, Instituto Alberto Luiz Coimbra de Pós-graduação e Pesquisa de Engenharia, Programa de Engenharia Civil, Rio de Janeiro, RJ, Brasil.

Submitted on May 24, 2024; Final Acceptance on January 13, 2025; Discussion open until August 31, 2025.
Editor: Renato P. Cunha
https://doi.org/10.28927/SR.2025.003824

strains is based on Buisman's formulation, which requires the secondary compression index $C_\alpha$. Other insights and formulations were put forward by Taylor (1942) and Leonards & Girault (1961), to mention just a few, and, more recently, in the works of Martins and colleagues (e.g., Martins, 2023; Oliveira et al., 2023; Santa Maria & Santa Maria, 2018).

PLAXIS solution for time-dependent deformation of clayey layers – Soft Soil Creep model – couples strain due to consolidation (strains associated with pore pressure dissipation) and due to creep (viscous strains). Consolidation strains follow Terzaghi's consolidation theory for pore pressure dissipation and creep strains are derived from a Buisman (1936)-type solution extended to three-dimensional conditions (Stolle et al., 1999). This is a model based on the isotache concept of Suklje (1957), and can be categorized under Hypothesis B of Ladd et al. (1977).

Although some numerical analyses of test embankments have been published (e.g., Huang et al., 2006; Mirjalili et al., 2012; Chai et al., 2013; Muthing et al., 2018), the present paper presents a 3D analysis of an embankment on heterogeneous ground, designed to induce large horizontal displacements, and includes a sensitivity study of the overall behaviour due to the parameters of the clayey layers.

In a case study, it is not possible to predict which contribution, between pore pressure dissipation (consolidation) and viscosity, is the most important, especially with layers at different depths. A sensitivity study such as the one presented here is necessary.

## 2. The test embankment

### 2.1 Location and geology

The test embankment was built in the Athletes' Village of the 2016 Olympic Games, in the Jacarepaguá Lowland, Rio de Janeiro. The local subsoil is characterized by a package of Holocene and Pleistocene sediments, originating from continental, sea, and lagoon deposits, consistent with the history of sea level variations. These deposits led to the formation of spits in this region, composed of low-density sands, peat, and soft plastic clays (Maia et al., 1984).

### 2.2 Geometry and instrumentation

Figures 1 and 2 show the embankment, geotechnical investigations and instrumentation in both plan and cross-section.

Before constructing the embankment, a geogrid was placed over the ground. The embankment had different slopes, with a steeper side reinforced with woven geotextile, in 0.5m thick layers. The purpose of this steeper slope was to induce high horizontal deformations in the ground, as part of a study of the effect of the embankment on nearby foundations. The material used was a sandy silt, with a natural unit weight of 19.5 kN/m$^3$ after compaction.

The instrumentation installed for monitoring the test embankment, shown in Figures 1 and 2, consisted of: (a) 3 settlement plates at the base of the embankment; (b) 4 electric vibrating wire piezometers installed in 4 verticals (totaling 16 piezometers) under the embankment and around it; (c) 2 inclinometer tubes.

## 3. Geotechnical investigation and geomechanical model of the ground

Field tests (SPT, CPTu, vane) and laboratory tests (oedometer, UU, CIU, CAU triaxials) were performed. Deformed samples extracted from the SPT sampler tip were subjected to lab tests for natural water content, fines content (passing through the No. 200 sieve), *LL* and *PL*. The location of the investigations can be seen in Figure 1.

The definition of stratigraphy – or geomechanical model of the ground – followed: (1) analysis of field and laboratory tests; (2) division of the subsoil into layers based on the results of these tests; (3) evaluation of the quality of the test results, where the good quality ones were selected to estimate the necessary parameters for the chosen soil behaviour models.

Based on the results of SPTs and CPTus, the subsoil was divided into 9 layers, up to the bedrock. Figure 3 shows the division of the profile based on SPT-03, while Figure 4 indicates the division based on Robertson's (1990) normalized parameters $Q_t$, $F_r$ and $B_q$ from CPTu-01, and also *Su* values from vane test VT-01, corrected for field conditions according to Bjerrum (1973).

The average points corresponding to the pairs ($Q_t$, $F_r$) and ($Q_t$, $B_q$) of each layer, obtained in CPTu-01, were taken to Robertson's (1990) charts for soil behaviour classification. Overall, this classification was in good agreement with the tactile-visual descriptions of the SPT samples. However, Layer 3 of peat could not be distinguished from Layer 4 of silty clay by CPTu-01. Its delimitation and classification as "peat" came from the tactile-visual descriptions of the SPT samples. Although the water content of Layer 3, around 100%, is low when compared to that of superficial peat in the Jacarepaguá Lowland, which can exceed 600% (Baroni, 2010), this difference can be explained by the compression of the peat caused by the 4m thick layer of sand overlying it, existing in the location for centuries according to the geological history of the region (Roncarati & Neves, 1976).

Figure 5 presents two sections, one across and the other along the axis of the embankment, showing the adopted division into layers.

As seen in Figure 1, the available geotechnical investigations are concentrated in the central region of the embankment and in front of its steepest slope, not covering its entire plan projection. As shown in the sections of Figure 5, in the space between the geotechnical investigations an interpolation of the geometry of the layers was carried

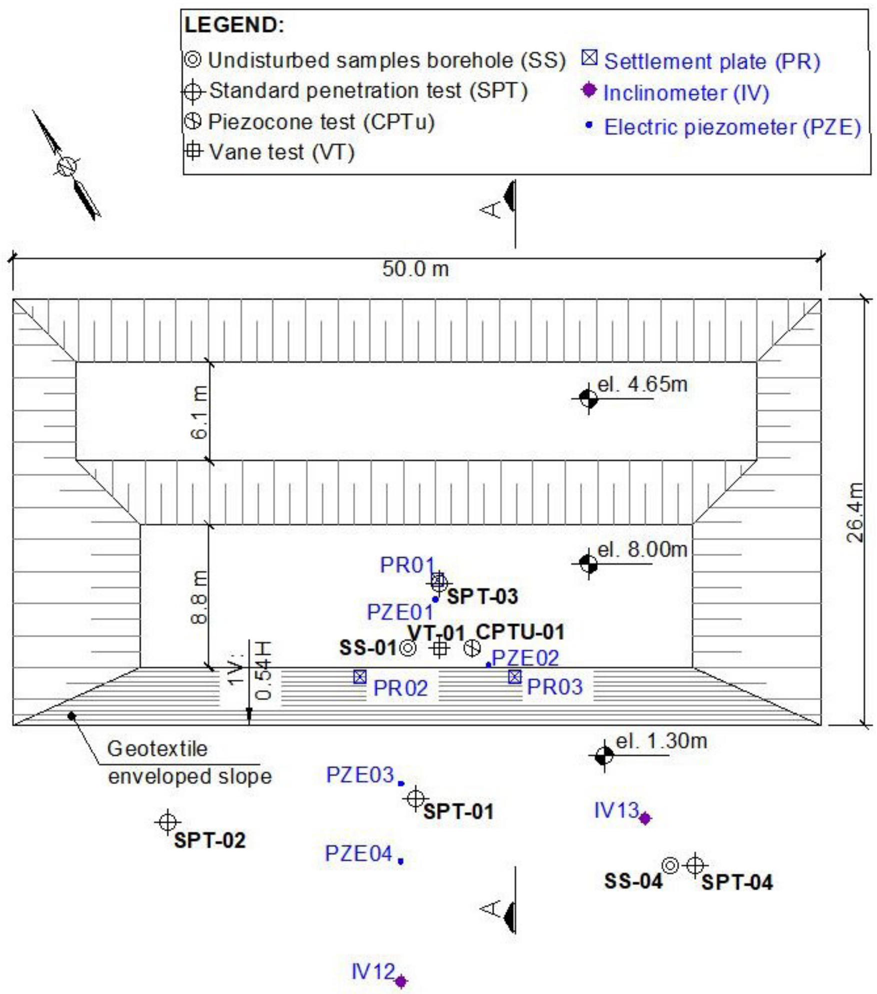


**Figure 1.** Plan view of the test embankment with investigations and instrumentation.

out, and externally a horizontal extrapolation was made as detected in the extreme investigation holes. On the one hand, the area of the natural ground subjected to greatest stress increases and where the instrumentation was installed is well defined by the geotechnical investigations. On the other hand, 4 CPTu profiles distant between 60m and 240m from the embankment indicate some heterogeneity of the ground, although in most of them soft clay layers (4, 5 and 7) and sand layer 6 were detected. Therefore, some heterogeneities where geotechnical investigations were extrapolated may occur, mainly variations in the location of free-draining layers, influencing the rate of pore pressure dissipation and settlements; the final settlements would be less affected, given the very similar thicknesses of the compressible layers. Horizontal displacements tend to be more affected than settlements by these possible inaccuracies.

To generate the volumes that model the soil layers in PLAXIS 3D, the option of providing the program with separation surfaces between the layers was used. Each surface was generated in the AutoCad Civil 3D software, with interpolation between points corresponding to the layer divisions of the cross and longitudinal sections shown in Figure 5. Some adjustments were necessary, through the addition of more interpolation points, in order to obtain a more realistic surface from a geotechnical viewpoint.

## 4. Soil models and parameters

For each soil layer, the most appropriate constitutive model was chosen, and a range of most likely values was defined for the necessary parameters. These ranges were defined after interpretation of field and laboratory tests and, in their absence, from correlations in the literature. Sensitivity studies were carried out, varying the parameters to the bounds of these ranges.

### 4.1 Soft clay layers

For the soft clay layers, the Soft Soil Creep model – SSC (described, for instance, in Stolle et al., 1999) was chosen

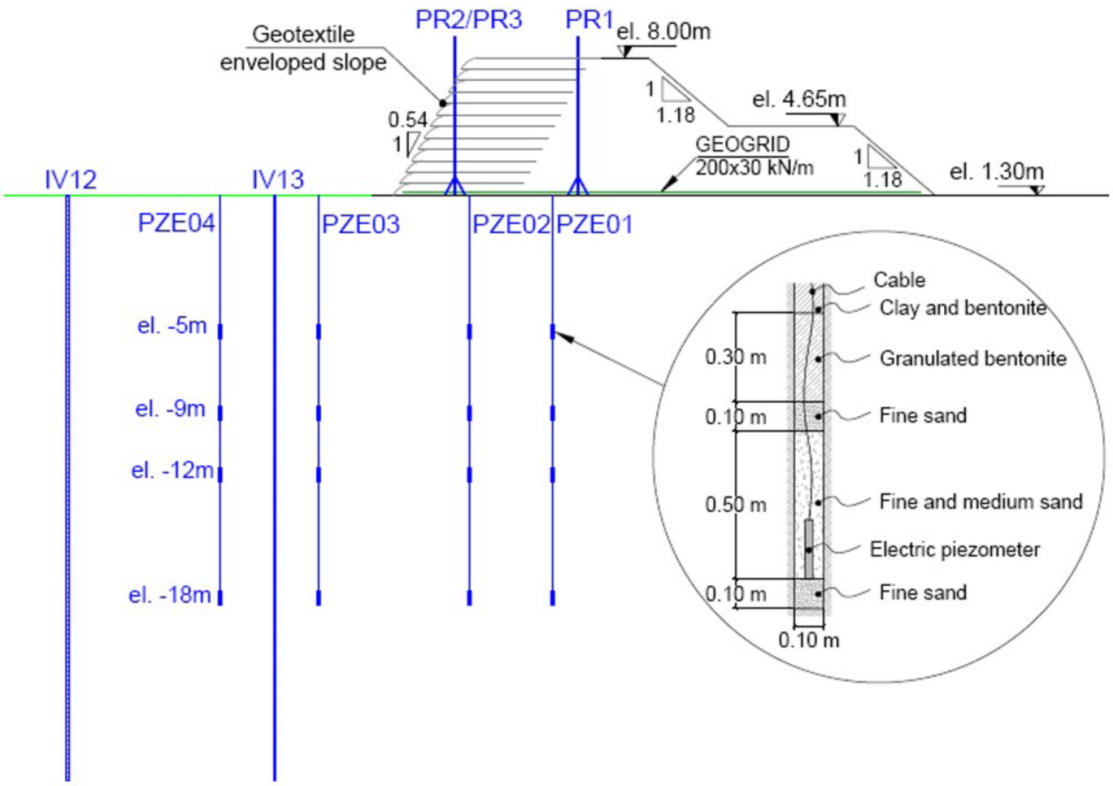


**Figure 2.** Cross-section AA indicated in Figure 1.

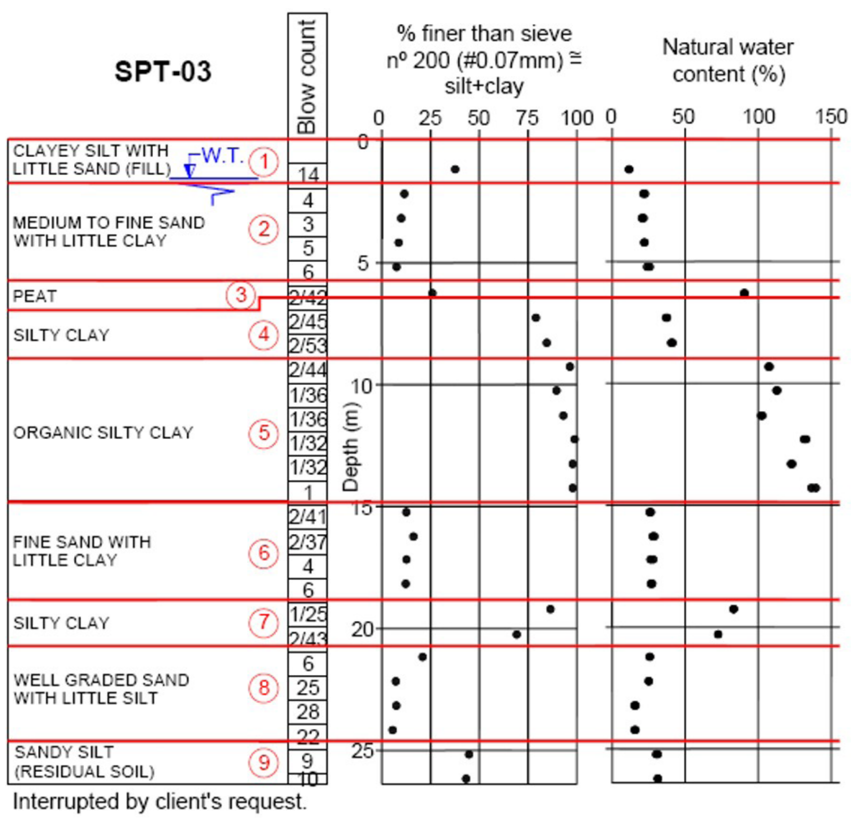


**Figure 3.** SPT-03 profile with indication of main soil layers.

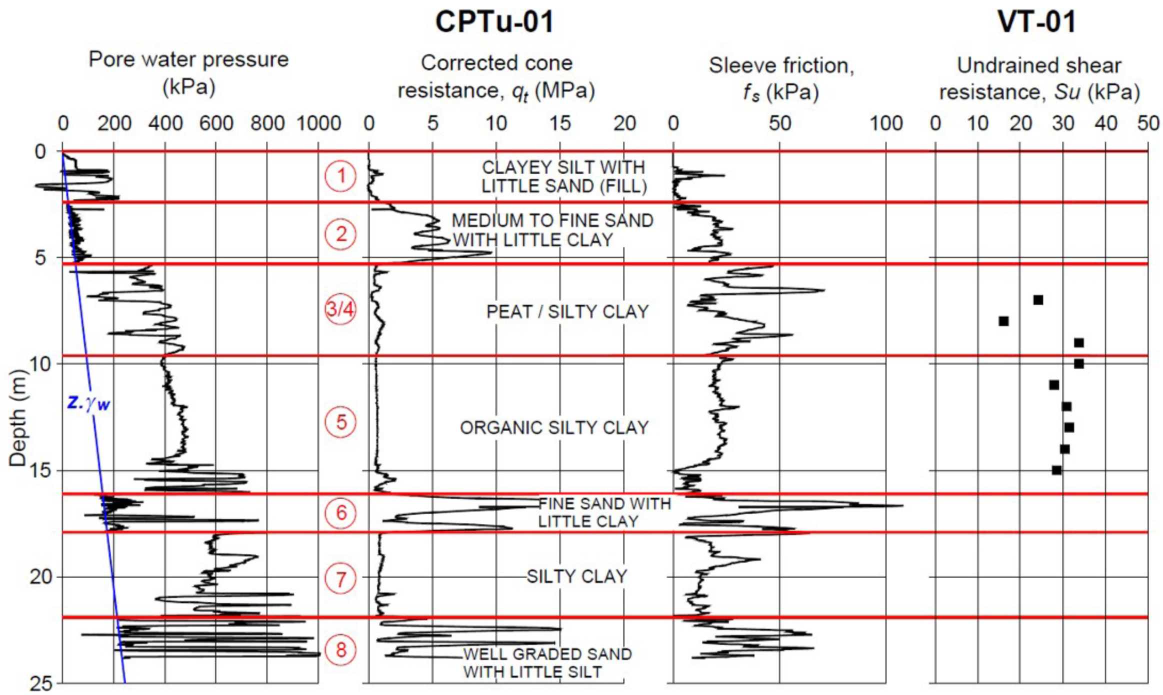


**Figure 4.** CPTu-01 and VT-01 results with indication of main soil layers.

as it allows the analysis of both primary and secondary consolidation (creep), important aspects in the present case.

Initially, the available oedometer tests were evaluated regarding the quality of the samples, based on the proposals of Lunne et al. (1997) and Coutinho (2007). Of the 16 available tests, 6 were classified as produced by good quality samples, all from Layer 5, with their curves $e$ vs. $\sigma'_v$ shown in Figure 6. The curves are similar, indicating very close values for $C_C$ and $C_S$, which were assigned to Layer 5.

For the other clay layers, $C_C$ was estimated from the correlation with the natural water content, $w_{nat}$, for soft clays of the Brazilian coastal region presented by Silva (2013), shown in Figure 7. In this figure, points from the 6 tests of the Athletes' Village fit well with local data by Baroni & Almeida (2017) and Almeida et al. (2013). For the definition of $C_S$, the same average value for $C_S/C_C$ of 0.08, obtained in the Layer 5 tests, was considered.

The oedometer tests and the geological history of the region indicate that the soft clay layers present overconsolidation due to aging, and an $OCR$ of 1.6, typical of the local soft clays (e.g., Baroni & Almeida, 2017), was adopted.

For the value of $\nu_{ur}$, related to the elastic behaviour in the unloading/reloading domain, there is little information in the literature (Kulhawy & Mayne, 1990), and the default value of PLAXIS equal to 0.15 was adopted.

The SSC model requires the use of the critical state friction angle $\phi'_{cv}$. Triaxial test results on a normally-consolidated specimen that reached the critical state indicated $\phi'_{cv} = 32º$, which was adopted for all clayey layers. As the clays are only slightly overconsolidated, $c' = 0$ was adopted.

As for the dilatancy angle $\psi$, for slightly overconsolidated soils, it can be considered equal to 0º.

For the earth pressure coefficient at rest, Jaky's (1944) expression for normally-consolidated soils was used, which, for the friction angle of 32º, led to $K_0^{nc} = 0.47$.

The initial values of the permeability coefficients in the three coordinated directions are necessary, in addition to the coefficient $c_k$, which defines their variation with the void ratio. For Layer 5, the values of $k_{z,init} = 1.0 \times 10^{-9}$ m/s and $c_k = 1.80$ ($e_{init} = 3.20$) were defined in order to have a reasonable adjustment to the $c_v$ values obtained in the oedometer tests shown in Figure 8 for the expected $\sigma'_v$ range (~ 50 to 220 kPa).

To estimate $k$ in the horizontal direction, CPTu dissipation tests were used. In Layer 5, the average $c_h$ value estimated using the method of Houlsby & Teh (1988) was $8.8 \times 10^{-7}$ m²/s. Danziger & Schnaid (2000) suggest that the $c_h$ value obtained through this methodology corresponds to the material in the recompression domain. When comparing this average value of $c_h$ with the average value of $c_v$ at recompression in oedometer tests, a ratio $c_h/c_v = 2.2$ is obtained, indicating $k_x = k_y = 2.2\ k_z$.

For the other clayey materials, the $k$ and $c_k$ values were estimated based on the mean $c_h$ values of the piezocone dissipation tests and on the following approximate relationships obtained for Layer 5:

$$c_v \cong c_h / 2.2 \tag{1}$$

$$c_{v,recompr} \cong 13 c_{v,virgin} \tag{2}$$

$$c_k \cong 0.6 C_c \tag{3}$$

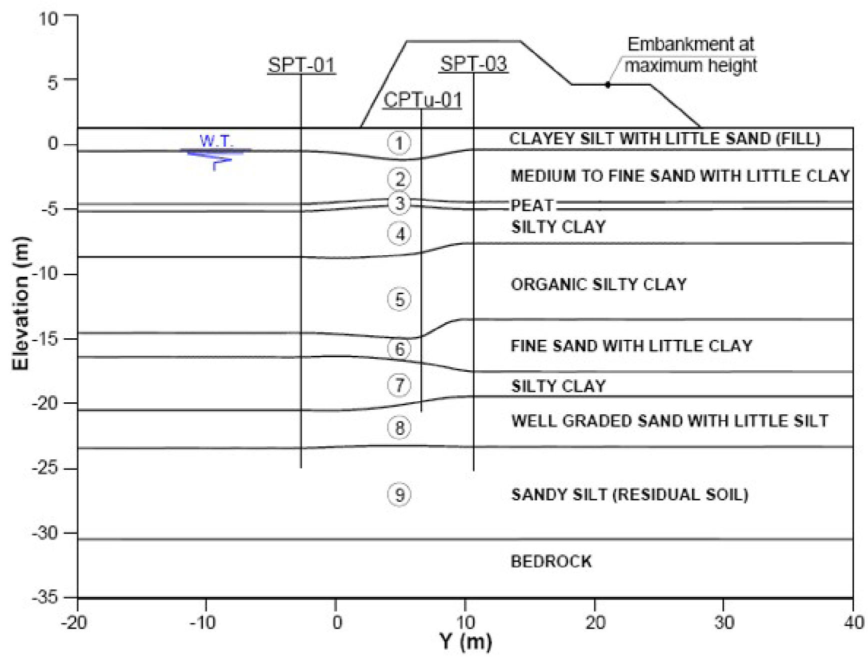


(a)

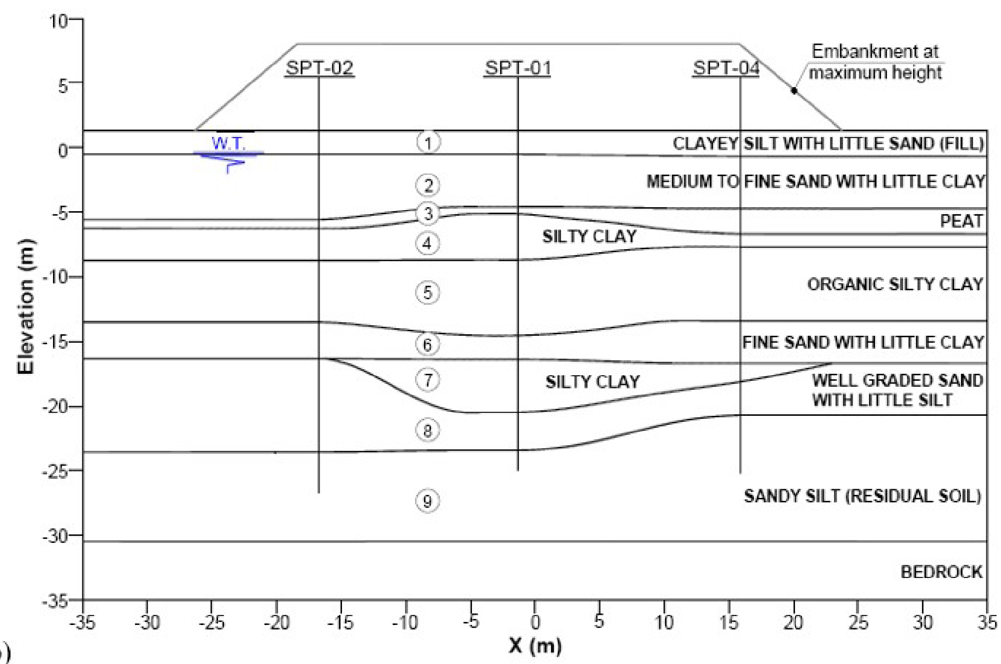


(b)

**Figure 5.** Ground profiles: (a) cross section and (b) longitudinal section.

The modified creep index $\mu^*$ can be obtained from the secondary consolidation (creep) index $C_\alpha$ with equation:

$$\mu^* = C_\alpha / \left[ \left( 1 + e_{init} \right) ln10 \right] \tag{4}$$

A $C_\alpha/C_C$ ratio equal to 0.05 was adopted for all clayey materials based on the results of oedometer tests and on typical values presented by Terzaghi et al. (1996).

Table 1 shows, for the clayey layers, the ranges of the parameters of the Soft Soil Creep model.

PLAXIS 3D has the SoilTest tool that allows the simulation of some laboratory tests with the specified parameters. Oedometer tests were simulated to check the $e$ vs. log $\sigma'_v$ curves, as exemplified in Figure 9a for Layer 5. It was observed that the simulated $C_C$ values

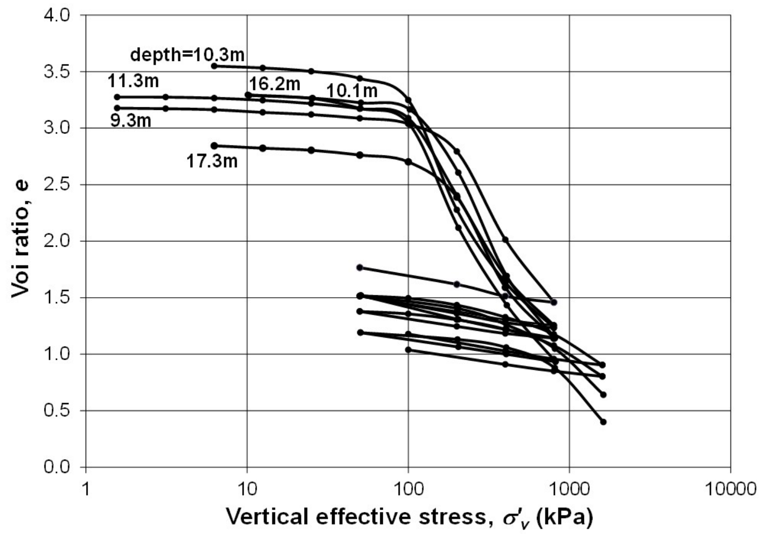


**Figure 6.** Oedometer compression curves of 6 good quality samples collected from Layer 5.

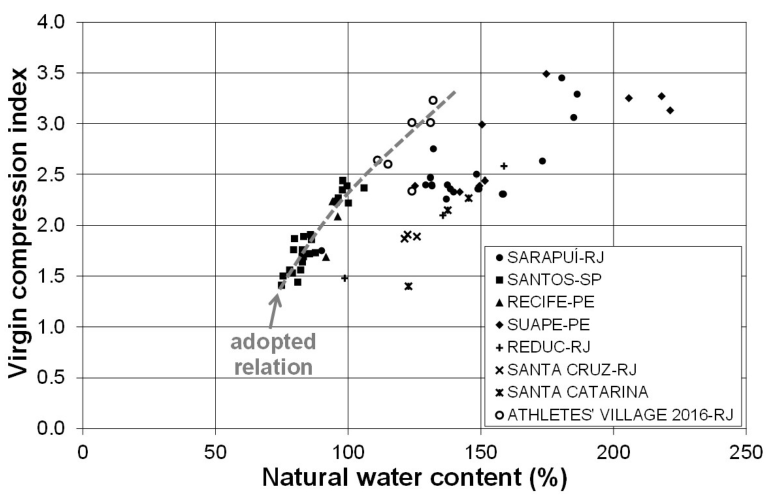


**Figure 7.** $C_C$ vs. $w_{nat}$ relation for high quality soft clay samples from the Brazilian coast (adapted from Silva, 2013).

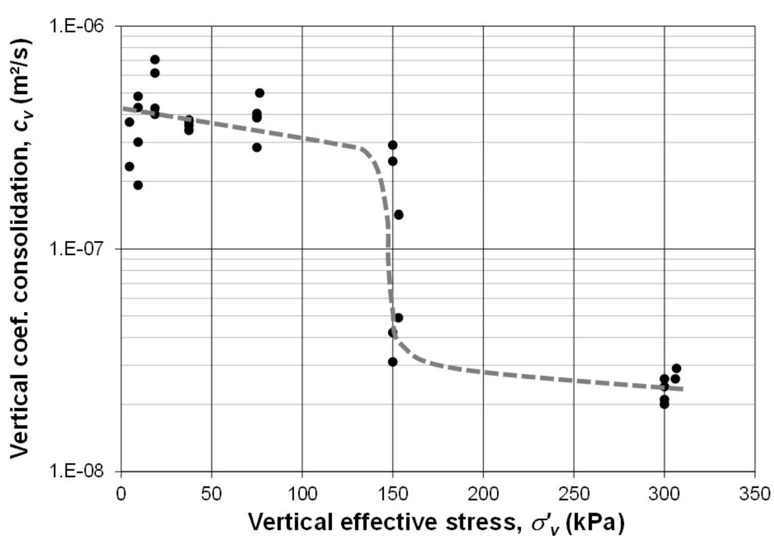


**Figure 8.** $c_v$ vs. $\sigma'_v$ data from oedometer tests on the best quality soft clay samples collected from Layer 5.

were consistent while simulated $C_S$ values were double the specified. This can be explained by the fact that the conversion from $C_S$ to $\kappa^*$, which is the parameter effectively used by the program, is not exact. For the program to consider the correct $C_S$ value, it was necessary to specify half of the values in Table 1.

The results of the triaxial tests – in which the critical state was reached – were compared with those simulated with the program, as exemplified in Figure 9b, with the following results:

- The $\sigma_d$ vs. $\varepsilon_a$ and $\sigma'_1/\sigma'_3$ vs. $\varepsilon_a$ simulated curves matched reasonably well with measurements; however, for

**Table 1.** Parameters of the Soft Soil Creep model for the clayey materials.

| Parameter | Layer 3 | | | Layer 4 | | | Layer 5 | | | Layer 7 | | |
|---|---|---|---|---|---|---|---|---|---|---|---|---|
| | min. | aver. | max. | min. | aver. | max. | min. | aver. | max. | min. | aver. | max. |
| $\gamma$ (kN/m³) | | 14.2 | | | 15.9 | | | 13.5 | | | 14.9 | |
| $e_{init}$ | | 2.6 | | | 1.6 | | | 3.2 | | | 2.1 | |
| $C_C$ | 2.10 | 2.35 | 2.60 | 1.20 | 1.50 | 1.70 | 2.70 | 3.00 | 3.20 | 1.30 | 1.60 | 1.90 |
| $C_S$ | 0.17 | 0.19 | 0.21 | 0.10 | 0.12 | 0.14 | 0.22 | 0.24 | 0.26 | 0.10 | 0.13 | 0.15 |
| $OCR$ | 1.3 | 1.6 | 1.9 | 1.3 | 1.6 | 1.9 | 1.3 | 1.6 | 1.9 | 1.3 | 1.6 | 1.9 |
| $v_{ur}$ | 0.05 | 0.15 | 0.25 | 0.05 | 0.15 | 0.25 | 0.05 | 0.15 | 0.25 | 0.05 | 0.15 | 0.25 |
| $c'$ (kPa) | | 0 | | | 0 | | | 0 | | | 0 | |
| $\phi'_{cv}$ | 24º | 32º | 40º | 24º | 32º | 40º | 24º | 32º | 40º | 24º | 32º | 40º |
| $\psi$ | | 0° | | | 0° | | | 0° | | | 0° | |
| $K_0^{nc}$ | 0.36 | 0.47 | 0.59 | 0.36 | 0.47 | 0.59 | 0.36 | 0.47 | 0.59 | 0.36 | 0.47 | 0.59 |
| $k_x = k_y$ ($10^{-9}$ m/s) | 9.3 | 37.4 | 112.2 | 6.6 | 26.4 | 79.2 | 0.5 | 2.2 | 6.6 | 0.3 | 1.2 | 3.6 |
| $k_z$ ($10^{-9}$ m/s) | 4.2 | 17.0 | 51.0 | 3.0 | 12.0 | 36.0 | 0.2 | 1.0 | 3.0 | 0.1 | 0.6 | 1.8 |
| $c_k$ | 0.19 | 1.41 | 2.35 | 0.12 | 0.90 | 1.50 | 0.24 | 1.80 | 3.00 | 0.13 | 0.96 | 1.60 |
| $C_\alpha$ | 0.12 | 0.14 | 0.16 | 0.06 | 0.08 | 0.09 | 0.12 | 0.15 | 0.18 | 0.06 | 0.08 | 0.10 |

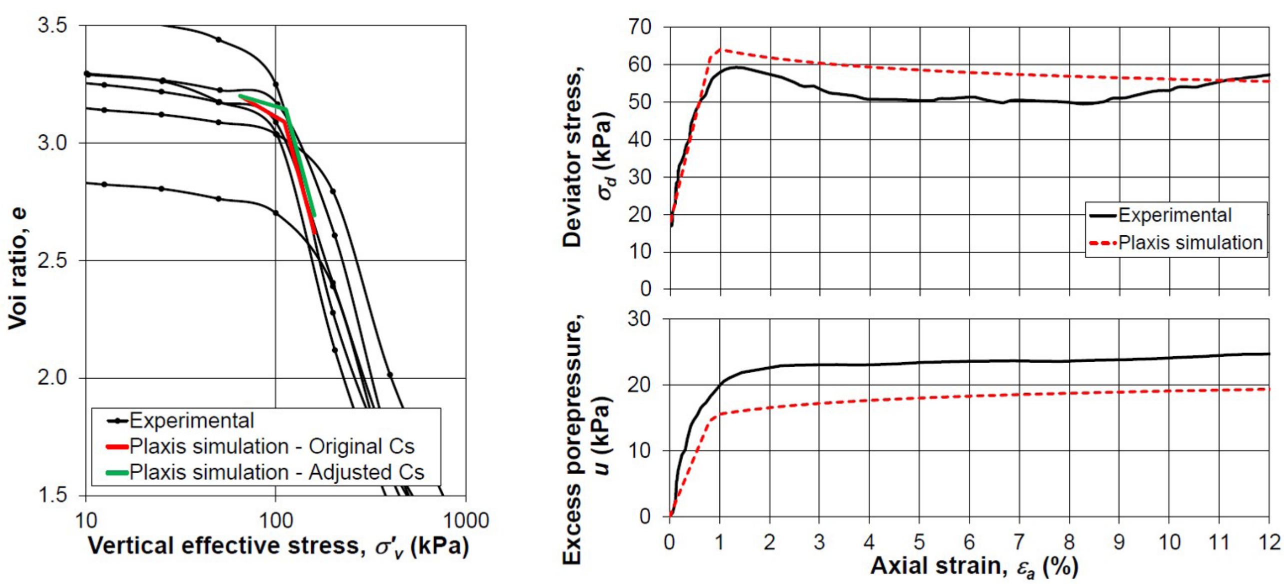


(a) (b)

**Figure 9.** Comparison between experimental and simulated results using the PLAXIS 3D SoilTest tool for Layer 5: (a) oedometer test and (b) CAU triaxial test.

some tests, they did not produce the peak observed in the measurements;
- The excess pore pressures simulated were underestimated by around 20%.

## 4.2 Sandy and silty layers

For the sandy and silty layers, the *Hardening Soil* model - HS (described, for instance, in Schanz et al., 1999) was chosen. Although not all parameters could be obtained directly from the appropriate tests, the HS model was considered the most suitable due to its consideration of the change in soil stiffness with the stress level and modeling of the loading history and also to the availability of correlations and typical values in the literature.

Layer 1 is a silty clay, compacted fill, classified as SM-SC by the Unified Soil Classification System, with an average $N_{SPT}$ value equal to 15, in which no field tests were carried out. Its parameters were estimated after the table of typical hyperbolic parameters for compacted Brazilian soils of Ehrlich & Becker (2010). For Layers 2, 6 and 8 the parameters were estimated mainly from correlations for granular soils with results of CPTu-01.

Layer 9 is a silty residual soil and was only reached by the SPT. After an estimate of $q_c$ values based on the correlations between SPT and CPTu results by Danziger & Velloso (1986), the same correlations of Layers 2, 6 and 8 were used.

For the HS model, the peak $\phi'$ is specified. The correlation of $\phi'$ with $q_c$ by Robertson & Campanella (1983) was used. A cohesion intercept $c' = 0$ was adopted for all materials. As for the dilation angle $\psi$, the following expression suggested by PLAXIS was adopted

$$\psi = \phi - 30^{\circ} \tag{5}$$

The proposals of Kulhawy & Mayne (1990) and Eslaamizaad & Robertson (1996) were used to estimate the tangent modulus $E_{oed}$ for the initial vertical effective stress, $\sigma'_{v0}$, from the cone resistance $q_c$. Subsequently they were converted to the values of $E_{oed}^{ref}$ relative to $\sigma'_v$ equal $p_{ref}$ = 100 kPa with an expression of the HS model.

Regarding the parameter $R_f$, which varies in a relatively narrow range, in the absence of CD triaxial tests, the typical value of 0.9 was adopted for all layers.

Although the original hyperbolic model uses the initial tangent modulus $E_i$, for PLAXIS, the equivalent parameter is $E_{50}$. These two parameters are related by the following equation:

$$E_{50} = E_i \left(1 - \frac{R_f}{2}\right) \tag{6}$$

The relation of $E_i$ to the confining stress (in the test) $\sigma_3$ follows (Janbu, 1963):

$$E_i = KP_a \left(\frac{\sigma_3}{P_a}\right)^n \tag{7}$$

The $K$ values were estimated through correlation with the friction angle proposed by Kulhawy & Mayne (1990). It was observed that the values of $E_{50}^{ref}$ thus estimated and $E_{oed}^{ref}$ had approximately the following relationship between them: $E_{50}^{ref} = 1.1\ E_{oed}^{ref}$, which agrees to the recommendation of PLAXIS to use $E_{50}^{ref} \sim E_{oed}^{ref}$.

As for the $E_{ur}^{ref}$ modulus, PLAXIS manual suggests $E_{ur}^{ref} = 3\ E_{50}^{ref}$. Duncan & Chang (1970) state that the $K_{ur}/K$ ratio ranges from 1.2 to 3.0, which, for $R_f = 0.9$, corresponds to the ratio $E_{ur}^{ref}/E_{50}^{ref}$ ranging between 2.2 and 5.5. Based on these two indications, it was adopted for all layers: $E_{ur}^{ref} = 3.5\ E_{50}^{ref}$.

Regarding the exponent $m$, which defines the dependence of stiffness ($E_{oed}$, $E_{50}$, $E_{ur}$) in relation to the confining stress level, the typical value for sands 0.5, was adopted for all layers in the absence of laboratory tests.

In the absence of laboratory tests, $\nu_{ur} = 0.2$ was adopted for all layers, following suggestion in the PLAXIS manual.

For the coefficient of earth pressure at rest in the normally consolidated condition, $K_0^{nc}$, the Jaky's expression (Jaky, 1944) was used. All silty and sandy materials were considered normally consolidated, except for Layer 1, which is a compacted material.

The mean values of $k$ were estimated from the grain size distribution, according to Cedergren (1967) and Robertson (1990).

Table 2 shows, for the sandy and silty layers, the ranges of the parameters of the Hardening Soil model.

## 4.3 Embankment

The focus of the analyses is on the subsoil's response to the applied surcharge, with no interest in the behaviour of the embankment body itself. Therefore, the simplest option would be to model the embankment as a distributed load applied to the ground surface, with the load value proportional to the embankment height at each point. However, the more rigid and resistant the embankment is in relation to the subsoil, the more the load distribution deviates from this pattern, tending to concentrate stresses in some regions. A more realistic option would be to separately model the compacted soil as an elastoplastic material, and the reinforcement elements (geotextiles and geogrids) using a specific model provided by PLAXIS 3D. The disadvantage of this option would be the likely occurrence of localized soil failures, which would make numerical convergence of the entire model difficult. Considering that these localized failures would not represent a general failure of the embankment due to the presence of reinforcement elements, it was considered an adequate option to model the embankment, together with its geotextiles and geogrid reinforcements, as an equivalent linear elastic material, with the parameters in Table 3. This approximation was considered satisfactory, bearing in mind the uncertainties of the stiffness and strength parameters of the compacted soil, on which no specific tests were available.

## 5. Parameter sensitivity studies with 2D model

PLAXIS 2D was used in the sensitivity studies due to its much shorter computation time compared to PLAXIS 3D (about 100 times less). In these studies, one parameter was varied at a time, the other parameters maintaining the average values of Tables 1 and 2. The parameter evaluated in an analysis was modified in all layers that had the same soil model. Two analyzes were performed for each parameter, one with the minimum, and the other with the maximum value of the range.

Figure 10 shows typical results of the sensitivity studies in the form of tornado-type graphs. They show the degree of relative influence that each parameter has on a given analysis result, ordered from top to bottom, from the most influential to the least influential, which is quantified by the length of the variation range of the specific result. The parameters in black correspond to layers with SSC model and the ones in red, to layers with HS model. The empty circles correspond to the lower value of the parameter range.

It can be observed that the parameters of layers with the HS model have little influence on the results when compared to those of the layers with the SSC model. The SSC parameters that most influence the results are, in order of importance:

- settlement at the end of monitoring: $k^{init}$, $c_k$, $OCR$
- horizontal displacements at the end of monitoring: $OCR$, $K_0^{nc}$, $k_{init}$, $c_k$, $\nu_{ur}$
- excess pore pressures: $OCR$, $k_{init}$, $C_\alpha$, $c_k$

In a similar sensitivity analysis, Muthing et al. (2018) verified the dominant influence of *OCR* on settlements. Here, the greatest influence of the permeability parameters is due to the fact that the settlements were compared at the end of the monitoring period, when not all excess pore pressures had dissipated, and not at the end of the consolidation process, when the influence of permeability would certainly be much less.

## 6. 3D modeling of the embankment

Figure 11 shows the 3D model created in PLAXIS 3D, with the embankment at its maximum height. The ground

**Table 2.** Parameters of the Hardening Soil model for the silty and sandy layers.

| Parameter | Layer 1 | | | Layer 2 | | | Layer 6 | | | Layer 8 | | | Layer 9 | | |
|---|---|---|---|---|---|---|---|---|---|---|---|---|---|---|---|
| | min. | aver. | max. | min. | aver. | max. | min. | aver. | max. | min. | aver. | max. | min. | aver. | max. |
| $\gamma$ (kN/m$^3$) | | 20.0 | | | 19.6 | | | 19.3 | | | 19.2 | | | 19.0 | |
| $e_{init}$ | | 0.50 | | | 0.60 | | | 0.60 | | | 0.68 | | | 0.71 | |
| $E_{oed}^{ref}$ (MPa) | 30 | 40 | 50 | 35 | 50 | 60 | 30 | 45 | 55 | 20 | 30 | 40 | 30 | 40 | 55 |
| $E_{50}^{ref}$ (MPa) | 33 | 44 | 55 | 39 | 55 | 66 | 33 | 50 | 61 | 22 | 33 | 44 | 33 | 44 | 61 |
| $E_{ur}^{ref}$ (MPa) | 116 | 154 | 193 | 135 | 193 | 231 | 116 | 173 | 212 | 77 | 116 | 154 | 116 | 154 | 212 |
| $m$ | 0.25 | 0.50 | 0.75 | 0.25 | 0.50 | 0.75 | 0.25 | 0.50 | 0.75 | 0.25 | 0.50 | 0.75 | 0.25 | 0.50 | 0.75 |
| $R_f$ | 0.70 | 0.90 | 0.98 | 0.70 | 0.90 | 0.98 | 0.70 | 0.90 | 0.98 | 0.70 | 0.90 | 0.98 | 0.70 | 0.90 | 0.98 |
| $OCR$ | | 2.0 | | | 1.0 | | | 1.0 | | | 1.0 | | | 1.0 | |
| $\nu_{ur}$ | 0.10 | 0.20 | 0.30 | 0.10 | 0.20 | 0.30 | 0.10 | 0.20 | 0.30 | 0.10 | 0.20 | 0.30 | 0.10 | 0.20 | 0.30 |
| $c'$ (kPa) | 20 | 30 | 40 | | 0 | | | 0 | | | 0 | | | 0 | |
| $\phi'$ | 33º | 36º | 39º | 39º | 42º | 44º | 32º | 38º | 42º | 27º | 32º | 37º | 32º | 35º | 40º |
| $\psi$ | 0º | 6º | 9º | 0º | 12º | 14º | 0º | 8º | 12º | 0º | 2º | 7º | 0º | 5º | 10º |
| $K_0^{nc}$ | 0.34 | 0.41 | 0.48 | 0.28 | 0.33 | 0.40 | 0.31 | 0.38 | 0.50 | 0.37 | 0.47 | 0.58 | 0.33 | 0.43 | 0.50 |
| $k$ ($10^{-6}$ m/s) | 0.2 | 2 | 20 | 5 | 50 | 500 | 1 | 10 | 100 | 50 | 500 | 5000 | 1 | 10 | 100 |
| $c_k$ | | $10^{15}$ | | | $10^{15}$ | | | $10^{15}$ | | | $10^{15}$ | | | $10^{15}$ | |

**Table 3.** Parameters for the embankment.

| Parameter | Value | Source |
|---|---|---|
| $\gamma$ (kN/m$^3$) | 19.6 | Average of in-situ tests |
| $E'$ (MPa) | 15 | Estimated, considering little compaction control |
| $\nu'$ | 0.3 | Estimated |
| $k$ (cm/s) | 1.0 x $10^{-3}$ | Estimated, considering a sandy silt |

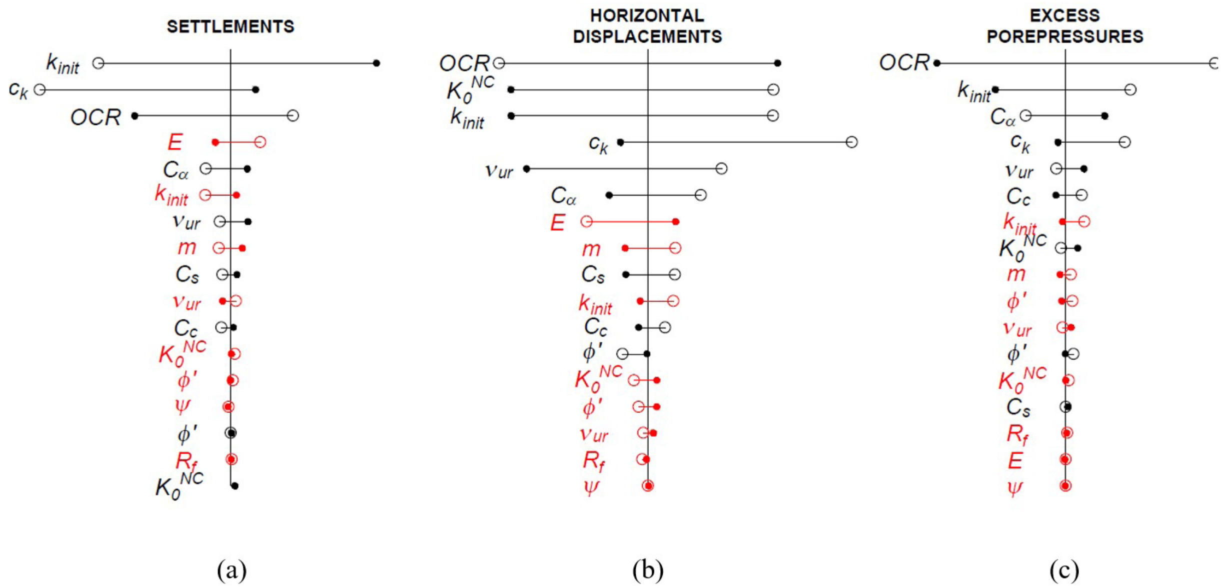


**Figure 10.** Sensitivity analysis: (a) settlements, (b) maximum horizontal displacements at the end of monitoring, and (c) excess pore pressures in Layer 5 at the end of embankment construction.

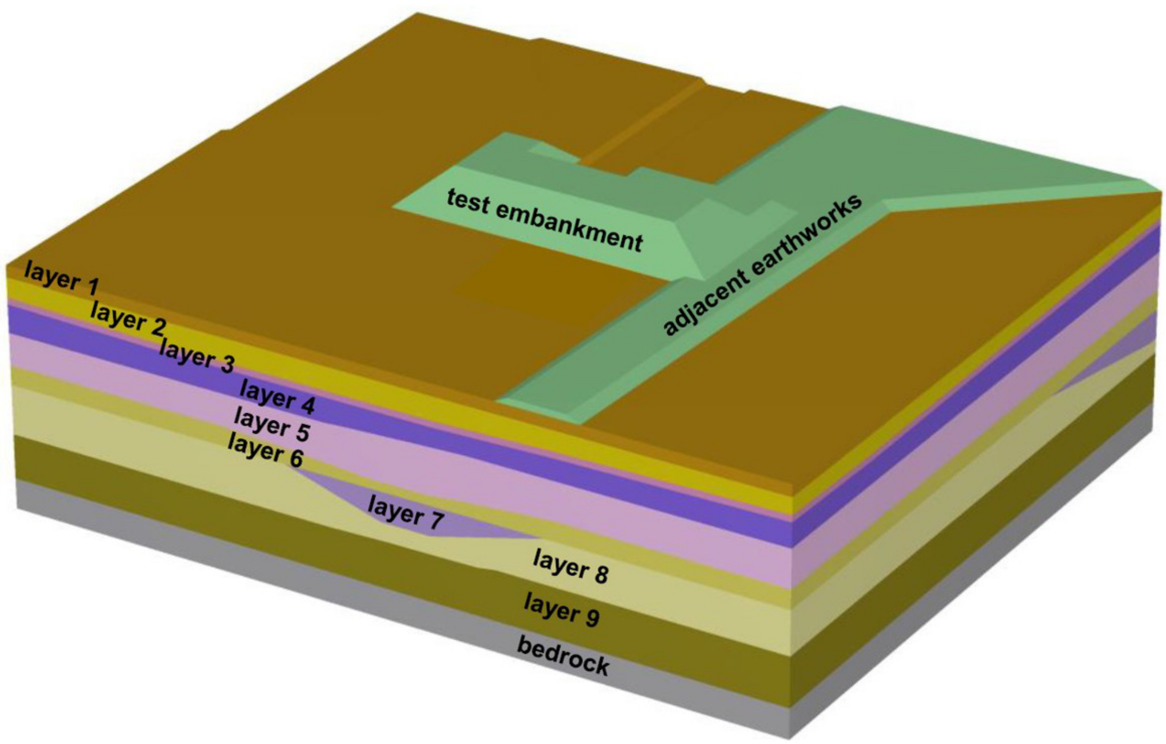


**Figure 11.** PLAXIS 3D model with the embankment at its maximum height.

was modeled with 120 x 100m plan dimensions, 36m deep. These dimensions were considered to be large enough to avoid the influence of prescribed boundary conditions (e.g., the maximum increase in vertical stress at boundaries is about 2% of the applied surface pressure).

The finite element mesh was generated by the software, resulting in the division of domain into 94630 ten-node tetrahedral elements, with average size around 2.3m. The prescribed boundary conditions were: on the four vertical faces, perpendicular displacements were prevented, and pore water could flow across; for the bottom, the displacements in the three directions were prevented and water flow was null.

### 6.1 Analysis sequence

Initial stresses were calculated through the PLAXIS K0-Procedure, based on the prescribed values of $K_0^{nc}$, *OCR*, and unit weight of each layer, considering the configuration that the ground presented before the construction of the Athletes' Village, which is presumed to have been the condition in which the site was for centuries, according to the history of the region.

For a more realistic simulation of the ground effective stresses states at the beginning of the test embankment, the modeling also included past earthworks carried out at the site and surrounding areas, which began approximately 16 months before the first raising of the embankment. These past stages were simulated using Consolidation type analyses, since the time elapsed until the beginning of the test embankment was not sufficient for the complete dissipation of excess pore pressures in the clayey layers, making it not possible to use a Drained type analysis.

The placing of layers of the test embankment were spaced from 2 to 5 days. These time intervals were not small enough to consider an undrained behaviour of the clay layers, which was confirmed by piezometers readings. Therefore, the process of raising the embankment was modeled in a Consolidation type analysis.

Since the number of readings on the inclinometers is very large (53 readings), comparisons between measured and computed horizontal displacements were made only for the following four dates/events:

- 04.Jul.2013: 4.5 days after the embankment reached 3.1 m;
- 15.Jul.2013: 5.5 days after the embankment reached 4.7 m;
- 31.Jul.2013: immediately after the embankment reached 6.7 m;
- 02.Sep.2013: last measurements.

In addition to raising the test embankment itself, other earthworks were carried out in its vicinity during the monitoring period, which were also considered in the model for more realistic results.

### 6.2 Final adjustment of parameters

After a 3D analysis with the average soil parameters, analyzes were performed again varying the parameters of the clay layers (the more influential parameters by the sensitivity studies). The analyses sought to improve matching of settlements measured by the settlement plates, which were underestimated, as well the horizontal displacements measured by inclinometers, which were overestimated.

In soft clays, the relationship between horizontal displacements and settlements in a 2D or 3D problem is strongly influenced by drainage conditions during load application: predominantly undrained loadings tend to generate greater horizontal displacements for a given value of settlement (due to the incompressibility of the soil in this condition) than drained loadings. Undrained displacements are directly derived from loading but may be increased by undrained creep, which is more significant the lower the factor of safety (Foott & Ladd, 1981). This behaviour can be observed in the sensitivity analysis presented in Figure 10b, where the lowest hydraulic conductivity value tested is associated with the greatest horizontal displacement. Therefore, the hydraulic conductivity of the clayey layers was the parameter that underwent the greatest adjustment. Furthermore, the pore pressure measurements (by piezometers) served to adjust parameters related to the rate of excess pore pressure dissipation.

The parameter adjustment was carried out by trying different values, guided by the sensitivity analyses, not using more advanced back-analysis techniques, as performed, for example, by Muthing et al. (2018).

Figures 12 to 14 show comparisons between measurements and analysis results, the initial analysis with average parameters in gray lines and final adjusted analysis in black lines. Due to similar behaviours, only the results of one settlement plate and one piezometer are presented.

The following observations can be made about the adjusted analyses:

1) Field measurements showed that the 3 settlement plates, despite being in different positions under the embankment, presented quite similar settlements (46, 45 and 44 cm on the last day of monitoring). The results of the adjusted analysis showed less uniform values, with settlements of 49, 39 and 41 cm on the last day. Nevertheless, for PR-1, central plate, the adjustment was quite satisfactory, with the difference between the calculated and the measured settlement of a maximum of +1 cm until 13.Aug.2013 and of +3 cm on the last day of monitoring (difference of + 6.5%). For PR-2 and PR-3, settlements were underestimated by the analysis.
2) The adjustment of the ground horizontal displacement profile was reasonable, since most profiles were within the uncertainty range of inclinometer measurements. For ground above Layer 7, there was no pattern in the deviations of the analysis in relation to the measurements: for certain depths/dates, horizontal displacements were overestimated and, for others, underestimated. From Layer 7 downwards, there was a general tendency to underestimate horizontal displacements, especially in the last monitoring dates.
3) As for excess pore pressures, it was observed that in absolute terms the results of the analysis were greater than those measured. In relative terms, it was observed that the difference between the computed

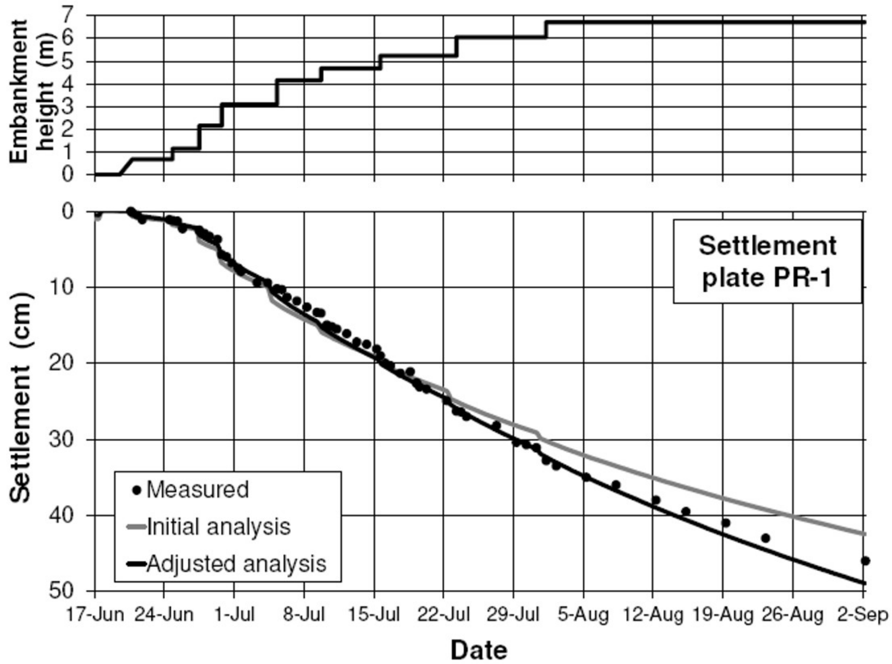


**Figure 12.** PR-1 settlement plate: measurements and results of both initial and adjusted analyzes.

and the measured values is approximately constant from 8.Jul.2013 onwards, which shows that the absolute differences observed are either due to the excess pore pressures values calculated before this date, or to the poor response of the piezometers due to a possible lack of saturation.

4) Despite the limited monitoring period, the model's ability to capture the field behaviour was on a par with other studies (e.g., Huang et al., 2006; Chai et al., 2013; Rezania et al., 2018), where good agreement is seldom obtained at the same time for settlements, horizontal displacements, and pore pressure development.

Table 4 shows the adjusted parameters of the clay layers in bold, with others initially defined. For a better adjustment of the settlement curves over time, the hydraulic conductivity values of Layers 5 and 7 were increased (6 and 3 times greater than the initial value). To reduce the horizontal displacements obtained in the initial analysis, in addition to increasing permeability, the $v_{ur}$ and $C_S$ values were also reduced.

For the other layers, the average parameters of Table 2 were maintained, with the exception of the strength parameters of Layer 1, that had to be increased to $c' = 50$ kPa and $\phi' = 38^{\circ}$ due to local failures that interrupted the numerical solution.

## 7. Long-term prediction

The test embankment was monitored up to 32 days after reaching its maximum height. In order to predict its long-term behaviour, the analysis was continued for another 50 years. Neither the reduction in the drainage distance of the clay layers (the option of updating the finite element mesh was not used) nor the load relief by submersion of the embankment were taken into account.

### 7.1 Long-term pore pressures and settlements

In the authors' understanding, the deformation process during clay consolidation is a visco-elasto-plastic phenomenon, as indicated by the mechanism devised by Terzaghi (1941) to explain the secondary effects of time. This secondary effect has a viscous nature and is an additional mechanism to Terzaghi's (1923) classical theory for one-dimensional consolidation. The mechanism suggests that film bonds are present in the contacts between the grains, made of viscous absorbed water, delaying the particles approximation, and that the deformations cease only after all contacts have transformed into solid bonds, which occur between the solid portions of the absorbed water layers.

As discussed by Oliveira et al. (2023), considering valid this mechanism, the distinction between primary compression and secondary compression only makes sense in the case of thin layers, such as in the oedometer test, where high strain rates mobilize a significant amount of viscous resistance during the so-called primary consolidation. This viscous resistance delays the compression process, and its demobilization occurs mainly after the excess pore pressure is essentially dissipated (which occurs in a short time due to the small thickness), generating the strains corresponding to the so-called secondary consolidation. In the case of thicker

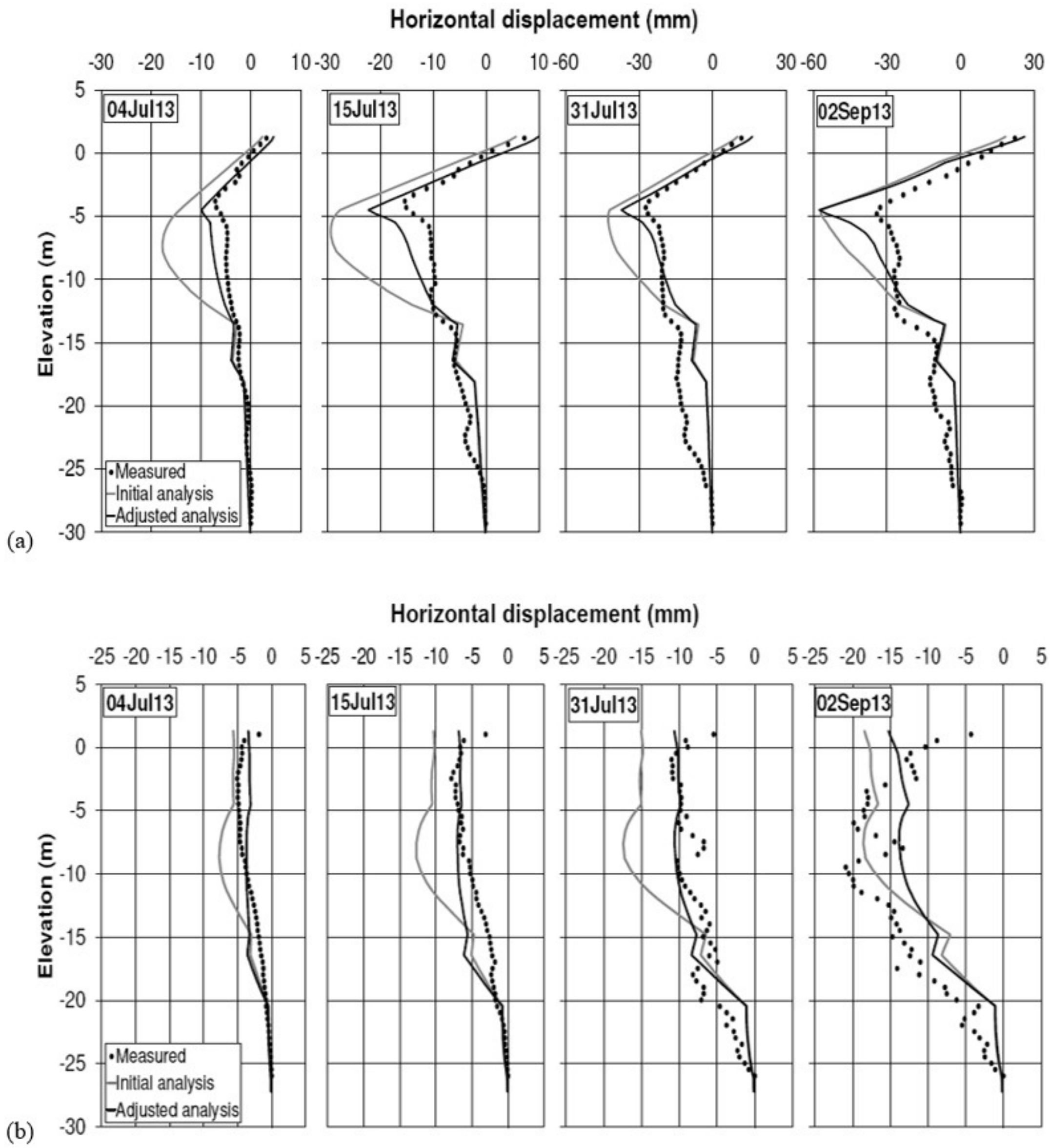


**Figure 13.** Measurements and results of both initial and adjusted analyzes: (a) Inclinometer IV-13; (b) Inclinometer IV-12.

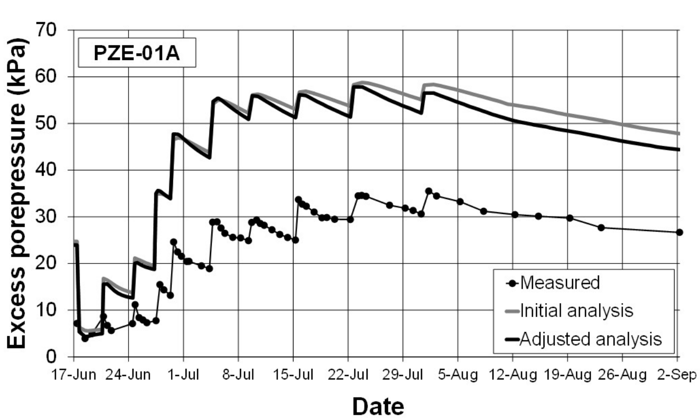


**Figure 14.** Piezometers at vertical PZE-01: measurements and results of both initial and adjusted analyzes.

**Table 4.** Adjusted parameters of the clay layers.

| Parameter | Layer 3 | | Layer 4 | | Layer 5 | | Layer 7 | |
|---|---|---|---|---|---|---|---|---|
| | initial | adjusted | initial | adjusted | initial | adjusted | initial | adjusted |
| $\gamma$ (kN/m³) | 14.2 | 14.2 | 15.9 | 15.9 | 13.5 | 13.5 | 14.9 | 14.9 |
| $e_{init}$ | 2.6 | 2.6 | 1.6 | 1.6 | 3.2 | 3.2 | 2.1 | 2.1 |
| $C_C$ | 2.35 | 2.35 | 1.50 | 1.50 | 3.00 | 3.00 | 1.60 | 1.60 |
| $C_S$ | 0.19 | **0.22** | 0.12 | **0.05** | 0.24 | **0.07** | 0.13 | 0.13 |
| $C_\alpha$ | 0.14 | 0.14 | 0.08 | **0.060** | 0.15 | **0.165** | 0.08 | **0.096** |
| $OCR$ | 1.6 | 1.6 | 1.6 | 1.6 | 1.6 | 1.6 | 1.6 | 1.6 |
| $v_{ur}$ | 0.15 | **0.05** | 0.15 | **0.05** | 0.15 | **0.05** | 0.15 | 0.15 |
| $c'$ (kPa) | 0 | 0 | 0 | 0 | 0 | 0 | 0 | 0 |
| $\phi'_{cv}$ | 32° | 32º | 32° | 32º | 32° | 32º | 32° | 32º |
| $\psi$ | 0° | 0° | 0° | 0° | 0° | 0° | 0° | 0° |
| $K_0^{nc}$ | 0.47 | 0.47 | 0.47 | 0.47 | 0.47 | 0.47 | 0.47 | 0.47 |
| $k_x = k_y$ ($10^{-9}$ m/s) | 37.4 | 37.4 | 26.4 | 26.4 | 2.2 | **13.3** | 1.2 | **4.0** |
| $k_z$ ($10^{-9}$ m/s) | 17.0 | 17.0 | 12.0 | 12.0 | 1.0 | **6.1** | 0.6 | **1.8** |
| $c_k$ | 1.41 | 1.41 | 0.90 | 0.90 | 1.80 | 1.80 | 0.96 | 0.96 |

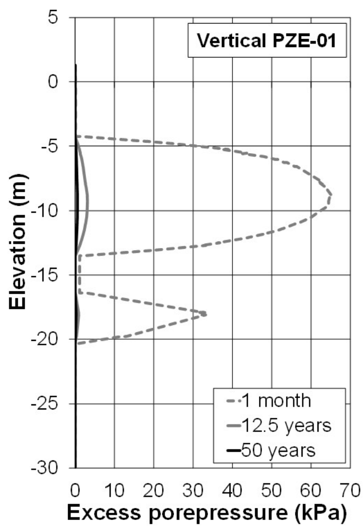


(a)

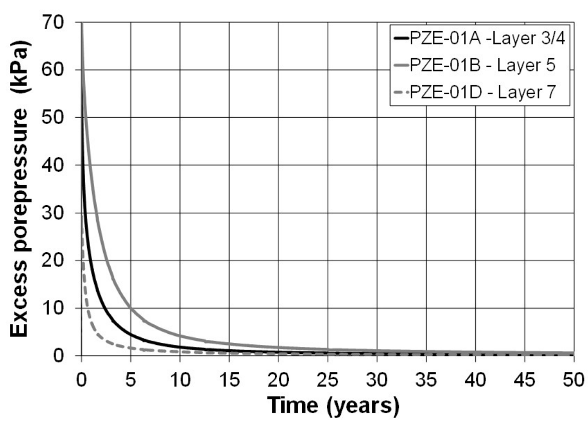


(b)

**Figure 15.** Excess pore pressures: (a) profiles at the vertical of PZE-01 and (b) development at piezometers' positions over time.

layers, such as those found in the field, the strain rates are very low, mobilizing little viscous resistance, so that there is practically no delay in the compression, which will occur during the pore pressure dissipation process (which develops slowly due to the great thickness). Thus, it is not divisible a period of primary compression and another of secondary compression, i.e., in field conditions, secondary consolidation occurs together with the primary consolidation.

In PLAXIS 3D, the soil model that comes closest to the behaviour described above, and that was adopted for clayey layers, is the Soft Soil Creep, which considers the occurrence of secondary consolidation (or creep) together with the primary consolidation, although it does not consider a final strain value for a given load (i.e., creep strains reduce logarithmically with time, but never cease).

Bearing in mind these considerations, which are important for simulations of long-term events, the model results follow.

Figure 15a presents the excess pore pressure profiles computed at the vertical of PZE-01 piezometers at different

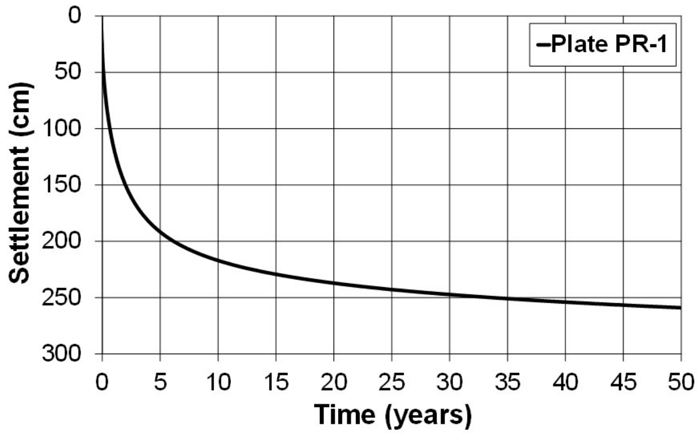


**Figure 16.** Settlement at the position of plate PR-1.

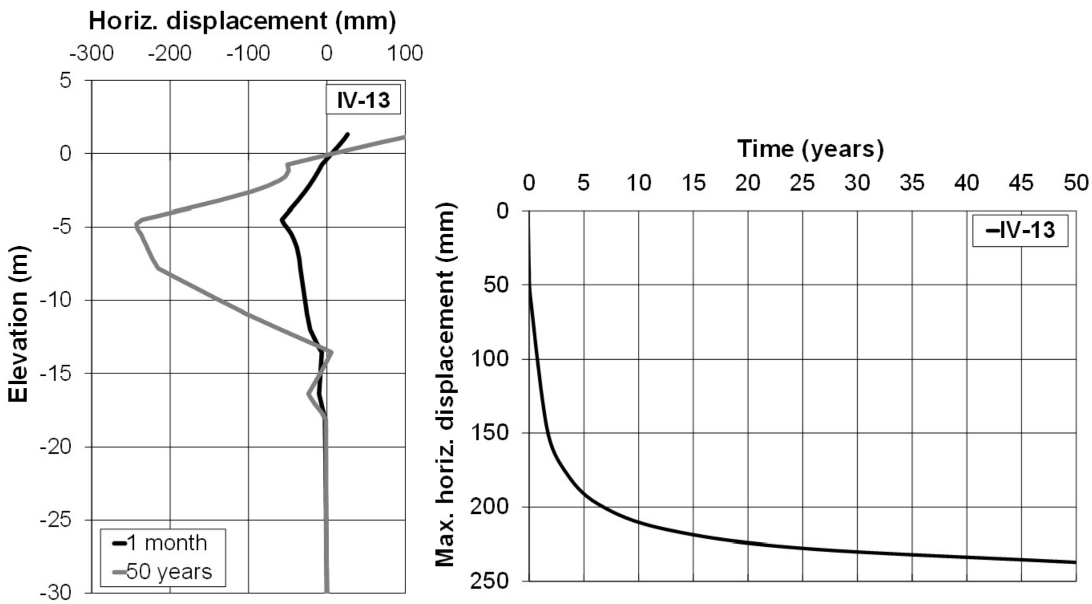


(a) (b)

**Figure 17.** Horizontal displacements in the IV-13 position: (a) profiles at different times and (b) development of the maximum horizontal displacement.

times after the end of the construction. Figure 15b shows the decrease of excess pore pressures over time in 3 piezometers. It is observed that, in the region of these piezometers, from 4 to 7 years after the last rise, 90% of excess pore pressures would have dissipated, and that 20 years later they would be practically null.

Figure 16 shows settlements of plate PR-1 over time, where it can be observed that, unlike excess pore pressures, there is no stabilization even after 50 years. This is due to the consideration of secondary consolidation in the Soft Soil Creep model adopted in the clay layers. Settlements after 50 years are about 2.5 times greater than those at 1 month after the final embankment rise.

### 7.2 Long-term horizontal displacements

Figure 17a shows horizontal displacement profiles at the inclinometer IV-13 position, on the last monitoring date (02.Sep.2013) and at the end of the 50-year analysis. Figure 17b shows the development of the maximum horizontal displacement, where it can be noted that it would quadruple in relation to those after 1 month of completing the embankment. And, as is the case of settlements, the horizontal ground displacements after 50 years would not be fully stabilized, due to creep.

## 8. Conclusions

1. The geotechnical investigations carried out at the test site allowed a good definition of the geometry of the subsoil layers, at least in the area subjected to the greatest stresses increase, consistent with the local geological history.
2. The sandy and silty layers were modeled in PLAXIS as Hardening Soil and the clayey layers as Soft Soil Creep. The former had their parameters estimated mainly from SPT, CPTu and correlations, while the latter from vane, oedometer and triaxial tests.
3. Sensitivity studies indicated that the parameters of the clayey layers were the ones that most influenced the analysis results, mainly the *OCR* and the permeability parameters.
4. The results of the initial 3D analysis of the embankment with the values for the parameters taken as the average of the probable range, agreed to some extent with the measured ground displacements. However, adjustments in the parameters of the clayey layers produced better predictions to both horizontal displacements, which had been overestimated, and settlements, which had been underestimated. Quantitatively, the average error in the settlements of PR-1 plate, for example, went from 12% in the initial analysis to 6% in the adjusted analysis, and the average error in the horizontal displacements in INC-13 inclinometer went from 214% to 169%.
   Regarding the excess pore pressures, although a good match with the piezometer measurements in absolute values was not achieved (analysis results being always higher than those measured), after a certain time, the incremental values came close, suggesting that the differences are due to the values calculated at the beginning of the monitoring, perhaps due to model inaccuracies, or possibly due to a lack of saturation of the piezometers.
5. Regarding the long-term behaviour, the analysis, extended to 50 years, indicated that:
   (i) after 20 years, excess pore pressures would be practically dissipated;
   (ii) even after 50 years, settlements and horizontal displacements would not be fully stabilized due to creep;
   (iii) at 50 years, settlements would be about 2.5 times greater than those at 1 month after the end of construction, and maximum horizontal displacements of the ground would be about 4 times greater.

## Acknowledgements

The embankment test was designed by Uberescilas F. Polido, Geoconsult. Hugo F. França performed/supervised most of the in situ and laboratory tests as part of his MSc research. The use of software PLAXIS 3D was made possible by Jean Pierre P. Rémy, Mecasolo Engineering. Prof. Marcio S.S. Almeida kindly reviewed the manuscript. CAPES - Coordenação de Aperfeiçoamento de Pessoal de Nível Superior, Brazil, partly financed this research under Finance Code 001.

## Declaration of interest

The authors have no conflicts of interest to declare. All co-authors have observed and affirmed the contents of the paper and there is no financial interest to report.

## Authors' contributions

Fernando da Silva Oliveira: conceptualization, methodology, formal analysis, visualization, writing – original draft. Francisco de Rezende Lopes: conceptualization, data curation, methodology, supervision, validation, writing – review & editing.

## Data availability

Data generated and analyzed in the course of the current study are available in the Civil Engineering Program - COPPE/UFRJ repository, http://www.coc.ufrj.br/en/master-dissertations/582-2015/5242-fernando-da-silva-oliveira.

## Declaration of use of generative artificial intelligence

This work was prepared without the assistance of any generative artificial intelligence (GenAI) tools or services. All aspects of the manuscript were developed solely by the authors, who take full responsibility for the content of this publication.

## List of symbols and abbreviations

| | |
|---|---|
| $c'$ | Cohesion intercept |
| $c_h$ | Horizontal coefficient of consolidation |
| $c_k$ | Coefficient of change of permeability |
| $c_v$ | Vertical coefficient of consolidation |
| $e_{init}$ | Initial void ratio |
| $f_s$ | Unit sleeve friction resistance |
| $k$ | Hydraulic conductivity |
| $m$ | Power for confining stress dependency of stiffness |
| $n$ | Modulus exponent |
| $p_a$ | Atmospheric pressure |

| | |
|---|---|
| $p^{ref}$ | Reference stress for stiffness |
| $q_c$ | Measured cone resistance |
| $q_t$ | Corrected cone resistance |
| $w_{nat}$ | Natural water content |
| $B_q$ | Pore pressure parameter, $(u_2-u_0)/(q_t-\sigma_{v0})$ |
| CAU | Consolidated anisotropically, undrained triaxial test |
| $C_C$ | Compression index |
| CIU | Consolidated isotropically, undrained triaxial test |
| CPTu | Cone Penetration Test with pore water pressure measurement |
| $C_S$ | Swelling/recompression index |
| $C_\alpha$ | Secondary compression index |
| $E'$ | Effective Young's modulus |
| $E_{50}$ | Secant stiffness in standard drained triaxial test |
| $E_i$ | Initial Young's modulus |
| $E_{oed}$ | Tangent stiffness for primary oedometer loading |
| $E_{ur}$ | Unloading/reloading stiffness |
| $F_r$ | Normalized friction ratio $= f_s/(q_t - \sigma_{v0})$ |
| $G_0$ | Initial shear modulus |
| $G_s$ | Secant shear modulus |
| $K$ | Dimensionless stiffness modulus |
| $K_0^{nc}$ | Coefficient of earth pressure in normal consolidation |
| $K_{ur}$ | Dimensionless unloading/reloading stiffness modulus |
| $LL$ | Liquid limit |
| $N_{SPT}$ | Blow count in the SPT |
| $OCR$ | Overconsolidation ratio |
| $PL$ | Plastic limit |
| $Q_t$ | Normalized cone resistance $= (q_t - \sigma_{v0})/\sigma'_{v0}$ |
| $R_f$ | Failure ratio $q_f/q_a$ |
| SPT | Standard Penetration Test |
| $Su$ | Undrained shear resistance |
| UU | Unconsolidated, undrained triaxial test |
| $\gamma$ | Unit weight |
| $\varepsilon_a$ | Axial strain |
| $\kappa^*$ | Modified swelling index |
| $\mu^*$ | Modified creep index |
| $\nu'$ | Drained Poisson's Ratio |
| $\nu_{ur}$ | Poisson's Ratio for unloading/reloading |
| $\sigma'_1$ | Major principal effective stress |
| $\sigma'_3$ | Minor principal effective stress |
| $\sigma_d$ | Deviator stress |
| $\sigma'_v$ | Vertical effective stress |
| $\psi$ | Dilatancy angle |
| $\phi'$ | Peak effective friction angle |
| $\phi'_{cv}$ | Critical state effective friction angle |

## References


Almeida, M.S.S., Riccio, M., & Baroni, M. (2013). Ground improvement in soft soils in Rio de Janeiro: the case of the Athletes' Park. *Proceedings of the Institution of Civil Engineers - Civil Engineering*, 166(6), 36-43. http://doi.org/10.1680/cien.13.00008.

Baroni, M. (2010). *Site investigation in very compressible soft clay deposits in Barra da Tijuca* [Master's dissertation, Federal University of Rio de Janeiro]. Federal University of Rio de Janeiro's repository (in Portuguese). Retrieved in May 24, 2024, from http://www.coc.ufrj.br/en/master-dissertations/306-2010/8230-magnos-baroni-2

Baroni, M., & Almeida, M.S.S. (2017). Compressibility and stress history of very soft organic clays. *Proceedings of the Institution of Civil Engineers - Geotechnical Engineering*, 170(2), 148-160. http://doi.org/10.1680/jgeen.16.00146.

Bjerrum, L. (1973). Problems of soil mechanics and construction on soft clays and structurally unstable soils (collapsible, expansive and others). In *Proceedings of the 8th International Conference on Soil Mechanics and Foundation Engineering* (vol. 3, pp. 111-159), Moscow.

Buisman, A.S.K. (1936). Results of long duration settlement observations. In *Proceedings of the 1st International Conference on Soil Mechanics and Foundation Engineering* (Vol. 1, pp. 103-106), Cambridge.

Cedergren, H.R. (1967). *Seepage, drainage, and flow nets*. John Wiley & Sons.

Chai, J., Igaya, Y., Hino, T., & Carter, J. (2013). Finite element simulation of an embankment on soft clay: case study. *Computers and Geotechnics*, 48, 117-126. http://doi.org/10.1016/j.compgeo.2012.10.006.

Coutinho, R.Q. (2007). Characterization and engineering properties of Recife soft clays - Brazil. In *Proceedings of the Second International Workshop on Characterisation and Engineering Properties of Natural Soils* (Vol. 3, pp. 2049-2100), Singapore. Balkema.

Danziger, B.R., & Velloso, D.A. (1986). Correlations between SPT and CPT results. In In *Proceedings of the VIII Brazilian Conference on Soil Mechanics and Foundation Engineering* (Vol. 6, pp. 103-113), Porto Alegre.

Danziger, F.A.B., & Schnaid, F. (2000). CPTu tests: recommendations and procedures. In *Proceedings of the IV Symposium on the Engineering of Special Foundations - SEFE* (Vol. 3, pp. 1-51), São Paulo (in Portuguese).

Duncan, J.M., & Chang, C.Y. (1970). Nonlinear analysis of stresses and strain in soils. *Journal of the Soil Mechanics and Foundations Division*, 96(5), 1629-1653. http://doi.org/10.1061/JSFEAQ.0001458.

Ehrlich, M., & Becker, L.B. (2010). *Reinforced soil walls and slopes: design and construction*. Taylor & Francis (in Portuguese).

Eslaamizaad, S., & Robertson, R.K. (1996). Cone penetration test to evaluate bearing capacity of foundation in sands. In *Proceedings of the 49th Canadian Geotechnical Conference* (pp. 429-438), St. John's. Canadian Geotechnical Society.

Foott, R., & Ladd, C.C. (1981). Undrained settlement of plastic and organic clays. *Journal of the Geotechnical Engineering Division*, 107(8), 1079-1094. http://doi.org/10.1061/AJGEB6.0001176.

Gray, H. (June, 1936). Progress report on research on the consolidation of fine-grained soils. In *Proceedings of the 1st International Conference on Soil Mechanics and Foundation Engineering* (Vol. 1, pp. 138-141), Cambridge.

Houlsby, G.T., & Teh, C.I. (1988). Analysis of the piezocone in clay. In *Proceedings of the International Symposium on Penetration Testing, ISOPT-1* (Vol. 2, pp. 777-783), Orlando. Balkema.

Huang, W., Fityus, S., Bishop, D., Smith, D., & Sheng, D. (2006). Finite-element parametric study of the consolidation behavior of a trial embankment on soft clay. *International Journal of Geomechanics*, 6(5), 328-341. http://doi.org/10.1061/(ASCE)1532-3641(2006)6:5(328).

Jaky, J. (1944). The coefficient of earth pressure at rest. *Journal of the Society of Hungarian Architects and Engineers*, 355-358.

Janbu, N. (1963). Soil compressibility as determined by oedometer and triaxial tests. In *Proceedings of the European Conference on Soil Mechanics and Foundation Engineering* (2 vol.), Wiesbaden.

Kulhawy, F.H., & Mayne, P.W. (1990). *Manual on estimating soil properties for foundation design - EL-6800, Research Project 1493-6, Final Report*. Cornell University - Geotechnical Engineering Group.

Ladd, C.C., Foott, R., Ishihara, K., Schlosser, F., & Poulos, H.G. (1977). Stress-deformation and strength characteristics. State-of-art report. In *Proceedings of the 9th International Conference on Soil Mechanics and Foundation Engineering* (Vol. 2, pp. 421-494), Tokyo.

Leonards, G.A., & Girault, P. (1961). A study of the one-dimensional consolidation test. In *Proceedings of the 5th International Conference on Soil Mechanics and Foundation Engeneering* (Vol. 1, pp. 213-218), Paris.

Lunne, T., Berre, T., & Strandvik, S. (1997). Sample disturbance effects in soft low plastic Norwegian clay. In *Proceedings of the Symposium on Recent Developments in Soil and Pavement Mechanics* (pp. 81-102), Rio de Janeiro. Balkema.

Maia, M.C.A., Martín, L., Flexor, J.M., & Azevedo, A.E.G. (1984). Holocenic evolution of the Jacarepaguá coastal plain. In *Proceedings of the XXXIII Brazilian Geology Conference* (pp. 105-118), Rio de Janeiro (in Portuguese).

Martins, I.S.M. (2023). The 8th Victor de Mello lecture: role played by viscosity on the undrained behaviour of normally consolidated clays. *Soil and Rocks*, 46(3), e2023006123. http://doi.org/10.28927/SR.2023.006123.

Mirjalili, M., Kimoto, S., Oka, F., & Hattori, T. (2012). Long-term consolidation analysis of a large-scale embankment construction on soft clay deposits using an elasto-viscoplastic model. *Soil and Foundation*, 52(1), 18-37. http://doi.org/10.1016/j.sandf.2012.01.010.

Muthing, N., Zhao, C., Holter, R., & Schanz, T. (2018). Settlement prediction for an embankment on soft clay. *Computers and Geotechnics*, 93, 87-103. http://doi.org/10.1016/j.compgeo.2017.06.002.

Oliveira, F.S., Martins, I.S.M., & Guimarães, L.J.N. (2023). A model for one-dimensional consolidation of clayey soils with non-linear viscosity. *Computers and Geotechnics*, 159, 105426. http://doi.org/10.1016/j.compgeo.2023.105426.

Rezania, M., Nguyen, H., Zanganeh, H., & Mahdi, T. (2018). Numerical analysis of Ballina test embankment on a soft structured clay foundation. *Computers and Geotechnics*, 93, 61-74. http://doi.org/10.1016/j.compgeo.2017.05.013.

Robertson, P.K. (1990). Soil classification using the cone penetration test. *Canadian Geotechnical Journal*, 27(1), 151-158. http://doi.org/10.1139/t90-014.

Robertson, P.K., & Campanella, R.G. (1983). Interpretation of cone penetration tests: part i: sand. *Canadian Geotechnical Journal*, 20(4), 734-745. http://doi.org/10.1139/t83-079.

Roncarati, H., & Neves, L.E. (1976). *Projeto Jacarepaguá - Estudo geológico preliminar dos sedimentos recentes superficiais da Baixada de Jacarepaguá, Município do Rio de Janeiro – RJ.* PETROBRÁS, CENPES, DEXPRO (in Portuguese).

Santa Maria, P.E.L., & Santa Maria, F.C.M. (2018). One-dimensional consolidation considering viscous soil behaviour and water compressibility – Viscoconsolidation. *Soils and Rocks*, 41(1), 33-48. http://doi.org/10.28927/SR.411033.

Schanz, T., Vermeer, P.A., & Bonnier, P.G. (1999). The hardening soil model: formulation and verification. In *Proc. Beyond 2000 in Computational Geotechnics – 10 Years of PLAXIS* (pp. 281-290). Balkema. http://doi.org/10.1201/9781315138206-27.

Silva, D.M. (2013). *Estimating the compression index of soft clays of the Brazilian coast from index tests* [Master's dissertation, Federal University of Rio de Janeiro]. Federal University of Rio de Janeiro's repository (in Portuguese). Retrieved in May 24, 2024, from http://www.coc.ufrj.br/en/master-dissertations/382-2013/4318-diego-moreira-da-silva

Stolle, D.F.E., Vermeer, P.A., & Bonnier, P.G. (1999). A consolidation model for a creeping clay. *Canadian Geotechnical Journal*, 36(4), 754-759. http://doi.org/10.1139/t99-034.

Suklje, L. (1957). The analysis of consolidation process by the isotache method. In *Proceedings of the 4th International Conference on Soil Mechanics and Foundation Engineering* (Vol. 1, pp. 200-206), London.

Taylor, D.W. (1942). *Research on consolidation of clays*. M.I.T. Department of Civil and Sanitary Engineering.

Terzaghi, K. (1923). *Die Berechnung der Durchlassigkeitsziffer des Tones aus Dem Verlauf der Hidrodynamichen Span-Nungserscheinungen* (pp. 125-138). Akademie der Wissenschaften in Wien, Mathematish-Naturwissen-SchaftilicheKlasse (in German).

Terzaghi, K. (1941). Undisturbed clay samples and undisturbed clays. *Journal of the Boston Society of Civil Engineers*, 28(3), 45-65.

Terzaghi, K., Peck, R.B., & Mesri, G. (1996). *Soil mechanics in engineering practice* (3rd ed.). John Wiley & Sons.